

Towards a Comprehensive Characterization of the Arrival Operations in the Terminal Area

Henrik Hardell

Communications and Transport Systems, ITN,
Linköping University (LiU), Norrköping, Sweden
Procedure Design Unit, Luftfartsverket (LFV),
Norrköping, Sweden, firstname.lastname@liu.se

Anastasia Lemetti, Tatiana Polishchuk, Lucie Smetanová

Communications and Transport Systems, ITN,
Linköping University (LiU)
Norrköping, Sweden
firstname.lastname@liu.se

Karim Zeghal

EUROCONTROL Innovation Hub,
Brétigny-sur-Orge, France
firstname.lastname@eurocontrol.int

Abstract—This paper aims at providing initial elements for a comprehensive characterisation of the arrival operations in the terminal area. It brings together different metrics, existing and new ones, and illustrates their application on three European airports operating with different metering and sequencing techniques (Dublin, Stockholm-Arlanda and Vienna). Precisely, the characterisation relies on three main flight efficiency metrics—horizontal and vertical deviations, and additional fuel burn—in relation to a metric capturing the entry conditions in the terminal area—the metering effort. The analysis is made on a selection of peak periods from 2019 with more than 5,000 flights in total, and relies on the data from the OpenSky Network.

The evaluation results uncover varied situations among the three airports. The median horizontal and vertical deviations range from 5 to 25 NM, and from 26590 to 30730 ft-minutes, respectively; and the median additional fuel burn from 96 to 176 kg. However, these values cannot be compared without considering the entry conditions to the terminal area. Here, for the peak periods, the metering effort is ranging from 1.2 to 3, reflecting very different entry conditions among the three airports. Further analysis would be required to study in more detail the arrival operations, in particular by considering comparable entry conditions.¹

Keywords—Arrival performance, flight efficiency, metering, terminal operations

I. INTRODUCTION

Terminal airspaces are the main contributors to inefficiencies in air traffic. The reasons are the complexity of the traffic in the Terminal Maneuvering Areas (TMAs) and airspace capacity limitations, negatively affecting the overall environmental footprint of the aviation sector. This work presents an approach targeting a comprehensive characterisation of the arrival operations in the terminal area. We use a set of performance metrics, existing and new ones, and illustrate their application on three European airports operating with different metering and sequencing techniques. We evaluate the arrival performance of Dublin, Stockholm-Arlanda and

¹This research is a part of the TMAKPI and ODESTA projects supported by the Swedish Transport Administration (Trafikverket). It is also supported via the IFWHEN project by the Swedish Transport Agency (Transportstyrelsen) and in-kind participation of LFV and EUROCONTROL.

Vienna airports, using the three main flight efficiency metrics: horizontal and vertical deviations, as well as additional fuel burn. Then we link the resulting performance to the metering effort indicator, capturing the entry conditions in the terminal area. An analysis per flow is also provided.

The rest of the paper is organised as follows: Section II presents previous work related to this paper. Section III describes the three airports, including runway configuration, arrival procedures and airspace. In section IV, the datasets used for our analysis are described. The methodology for evaluation of the arrival performance is given in Section V. We present the results in Section VI and conclude the paper with Section VII.

II. RELATED WORK

Evaluation of flight efficiency, and in particular TMA performance, has been a topic of interest in recent years. International Civil Aviation Organization (ICAO) proposed a set of metrics to enable analysis of TMA performance [1]. EUROCONTROL developed the methodology used by its Performance Review Unit (PRU) for the analysis of flight efficiency within the areas of safety, capacity, cost-effectiveness and environment, reflected in the yearly assessment reports, reviewing the flight inefficiency within TMA at the top 30 European airports [2].

Pasutto et al. [3] analyzed the factors affecting vertical efficiency in descent, with the aim to determine where exactly the inefficiencies occur. They developed a method to isolate and quantify the respective contributions of airspace versus operations, with the varying horizon around the airport. The studies confirm that the airspace is generally the main source of inefficiencies, due to the complexity in and around these terminal areas. The authors proposed to combine the deviation from the ideal vertical profile and the time into one metric, which we adopted and slightly modified in this work.

Estimation of the flight inefficiencies in terms of extra fuel burn calculated based on the algorithm proposed in [4] was considered in the scope of APACHE project [5]. Later Prats et

al. [6] proposed a family of performance indicators to measure fuel inefficiencies.

In [7] fuel consumption is evaluated for terminal areas with a Terminal Inefficiency metric based on the variation in terminal area fuel consumed across flights, reported by a major U.S. airline. Furthermore, in [8] and [9], fuel savings of the Continuous Descent Operations (CDO) with respect to conventional procedures are analyzed. The works report the reduction in fuel consumption of around 25-40% when flying CDOs.

An analysis of the arrival flight efficiency at Stockholm-Arlanda airport in 2019 and 2020 was presented in [10] and [11]. In this paper, we extend and complement the methodology presented in these works, applying it to Arlanda and two other European airports with different TMA complexities and arrival procedures.

III. AIRPORTS

Two of the possible ways to facilitate sequencing along the dedicated route structures are trombone and point merge procedures. Point merge has been deployed relatively recently in Oslo, Dublin and other airports around the globe [12].

For our analysis, we choose three airports with different sequencing and merging techniques: open-loop vectoring at Stockholm-Arlanda (ESSA), trombone at Vienna (LOWW), and point merge procedures at Dublin (EIDW). All the three airports have similar number of yearly movements, between 220,000 and 270,000.

A. Runway Configuration

The runway configurations at the three selected airports differ, both in terms of layout and count. Dublin has two intersecting runways, but since runway 16/34 is only used for 5% of the aircraft movements, the two runways are rarely used simultaneously. Hence, Dublin can be considered a single-runway airport.

Arlanda has three runways in total, and most of the times, one runway is used for takeoffs and another for landings. The parallel runways is the preferred pair during peak hours and the capacity is 80 movements per hour.

Vienna has two intersecting runways that are used simultaneously to split the departures and arrivals. The runway capacity at Vienna is 68 movements per hour.

B. Arrival Procedures

Dublin operates point merge procedures for both directions to its main runway 10R/28L, and Standard Arrival Routes (STARs), without point merge, to the intersecting runway 16/34. The point merge procedures published for runway 28L are shown in Figure 1a [13]. Point merge procedures are designed to work in high-traffic loads without radar vectoring, and consists of a merge point and a set of sequencing legs flown at level, used for path stretching, before the aircraft are instructed to go direct to the merge point [12].

Arlanda operates a mix of closed STARs that connect all the way to the final approach, and open STARs, that

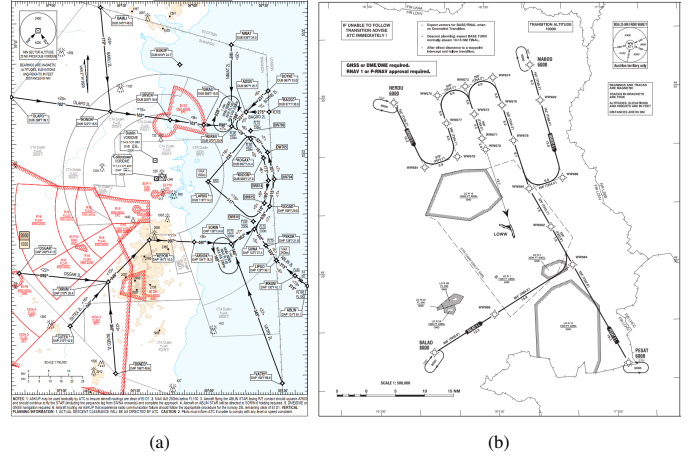


Figure 1. Published point merge procedures at Dublin runway 28L (a) and trombone procedures at Vienna runway 16 (b) (Sources: Irish AIP [13] and Austrian AIP [14]).

require vectoring by the air traffic controllers from the Initial Approach Fix (IAF) to the final approach. The only runway not having a closed STAR system is 01R/19L.

Vienna operates a set of STARs that lead to one out of four IAFs, shared by all four runways. From each IAF, a trombone transition connects to the final approach. The trombone procedures published for runway 16 are shown in Figure 1b [14]. The waypoints in the trombone system are used to adjust the path of the aircraft, in order to achieve the desired sequencing and separation. In reality, the turn to final is achieved by vectoring.

C. The TMAs

Stockholm Arlanda TMA is the largest TMA in the East-West direction, while all three TMAs are about the same size in the North-South direction. For Arlanda and Vienna, there are four published points for TMA entry, and in Dublin TMA there are 10. The three TMAs are shown in Figure 2.

Stockholm and Dublin have TMA borders defined by a limited number of coordinates, while parts of the Vienna TMA border follows the state border to other countries. Hence, we simplified those parts of the TMA by connecting some of the TMA edges with straight lines.

Our initial idea was to evaluate the performance inside TMA only, but after analyzing the actual arrival flows at all three airports, we noticed that a significant part of the descent phase of the eastbound arrivals to Dublin airport are cut, since the eastern TMA border is too close to the runway. For that reason, we extended our area of interest for Dublin to a 50 NM circle centered at the airport, combining the two approaches (see Figure 2a). For simplicity, the 50 NM circle area around Dublin airport will still be referred to as TMA.

IV. DATASETS

For the flight trajectories, we rely on the historical database of the OpenSky Network [15], [16], which provides an open-source data in a form of aircraft state vectors for every second

of the trajectories inside the terminal area. The data is transmitted by the Automatic Dependent Surveillance Broadcast (ADS-B) aircraft transponders, and collected via sensors on the ground, supported by volunteers, industrial supporters, and academic or governmental organizations. The applicability of this type of data for performance assessment purposes is justified in [17].

A cleaning and filtering was however required to remove any incomplete or erroneous records and non-typical flights. This includes removing fluctuations in latitude, longitude or altitudes, smoothing of altitude inconsistencies with Gaussian filter, removing incomplete or too damaged trajectories, removing flights such as: go-arounds, not landing on the runway, departure and arrival at the same airport (mostly helicopters), most non-commercial. The resulting dataset contains only complete aircraft trajectories from the terminal area entry until landing, representing the normal operations.

We consider the year 2019 and select four full weeks in October, which was the month with the highest number of arrivals at the three airports. 8797 arrivals at Dublin, 8132 at Arlanda and 9625 at Vienna airport. For each airport, we select the most used runway: 16 for Vienna (4192 arrivals – 44%), 01R for Arlanda (2830 arrivals – 35%), and 28L for Dublin (7741 arrivals – 88%). Then, for each of the three airports we created datasets based on Time in TMA, containing the arrivals, which spent significantly long time in TMA. For each airport, we calculated average per hour Time in TMA and removed 0.7 percentile from this set of values. The rest of the values correspond to the hours, which represent the peak time periods and contribute to the dataset for the corresponding airport. The resulting datasets contain 2587 flights for Dublin, 1045 for Arlanda and 1641 for Vienna.

V. METHODOLOGY

The proposed characterisation of the arrival operations relies on three main flight efficiency metrics—horizontal and vertical deviations, and additional fuel burn—in relation to a metric capturing the entry conditions in the terminal area—the metering effort. The horizontal and vertical deviations, as well as the metering effort, are derived from the metrics developed by Eurocontrol PRU and the Innovation Hub (formerly the Experimental Centre) [18], [19].

A. Horizontal Flight Efficiency

The horizontal flight efficiency is assessed through the horizontal deviation from a reference trajectory, here measured as a distance and denoted also **Additional Distance**. We have considered as a reference an ideal trajectory, which encompasses both airspace and operations related inefficiencies [20], [21]². The starting point is to identify arrival flows by clustering the flown trajectories as proposed in [20]. Then a user-preferred route tree is constructed as defined in [22]. We identify the start of the reference trajectory as the point on the TMA border as the closest to each cluster centroid. The reference

²Due to the rather limited traffic sample, we preferred not to rely on the notion of statistical best performers used to assess the operations inefficiencies.

trajectory goes directly to the current interception point and altitude of the localizer, with a 2 NM straight segment before the Final Approach Point (FAP). Figure 2 shows the reference trajectories per arrival flow (cluster) in black, for all three airports together with the actual arrival trajectories colored according to their relation to different clusters. It is clear from the figures that all these ideal references would not enable a structuration of the arrival routes facilitating an easy integration of the flows. That is in essence the purpose of this notion of the ideal references: to capture the cost of the route structuration, as well as the cost of the path stretching for sequencing.

In addition, we introduce the metric of **Horizontal Spread** to estimate the surface of the terminal area occupied by the flights and to quantify the dispersion of the arrival flows. It is calculated as the ratio of the number of cells through which at least one trajectory passes to the total number of grid cells covering the TMA. (Here we refer to the grid used for the construction of the minimum time to final heatmap, explained later in Subsection V-D). Smaller Horizontal Spread indicates that the aircraft trajectories lie not that far from each other and mainly follow similar arrival paths.

B. Vertical Flight Efficiency

The vertical flight efficiency is assessed through the Vertical Deviation from a Reference Profile, and complemented by the Time Flown Level.

The **Time Flown Level** is calculated using the technique proposed by EUROCONTROL in [18] with small changes. We identify the point of the trajectory in which the aircraft enters the TMA and use it as a starting point for the calculations. We identify a level segment when the aircraft is flying with the vertical speed below 300 feet per minute at least 30 seconds, and these 30 seconds are subtracted from each level duration as suggested in [18]. The flights under 1000 feet, corresponding to the final approach, are not considered as level flights.

For the **Vertical Deviation**, the reference profile is a continuous descent, constructed following the methodology proposed in [23], using Eurocontrol Base of Aircraft Data v 4.2 [24]. Figure 3 illustrates vertical profiles for several example clusters at each airport and the reference CDOs. For each flight, we create two different CDOs, called Reference Trajectory 1 (RT1) and Reference Trajectory 2 (RT2). The two trajectories only differ in the lateral distance, with RT1 following the same horizontal trajectory as the real flight, and RT2 following the horizontal trajectory of the reference trajectory explained in Section V-A. Thus, in most cases, RT2 will have a shorter horizontal trajectory than RT1, and since the horizontal trajectory of RT1 is identical to that of the real flight, it will also include any path extension (e.g. vectoring, holding patterns) performed by the aircraft, but still continuously descending. Note that the CDO trajectories designed in [23] are similar to the RT1 trajectories. Figure 4 shows the horizontal and vertical trajectories for an example flight for RT1 and RT2. As can be seen, the vertical profile is almost identical for RT1 and RT2, the only difference being

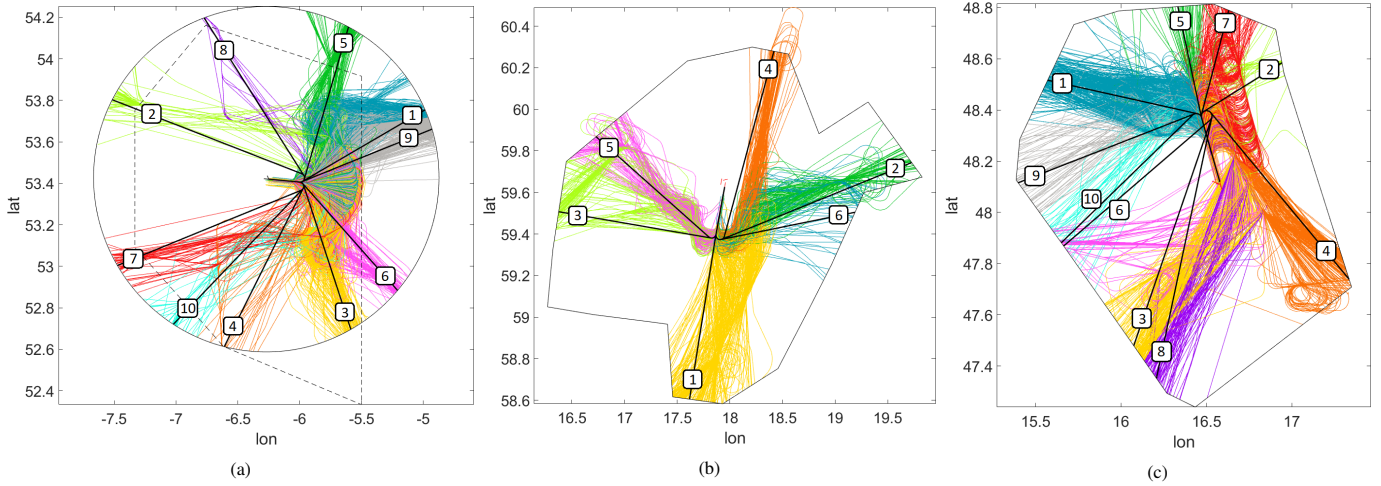


Figure 2. Horizontal reference trajectories (black lines) and the actual arrival trajectories colored by cluster, for EIDW (a), ESSA (b) and LOWW (c). For ESSA and LOWW, the area of interest is bounded by the actual TMA border, while for EIDW, the area is defined by a 50 NM radius circle, and the actual TMA border is illustrated by the dashed line.

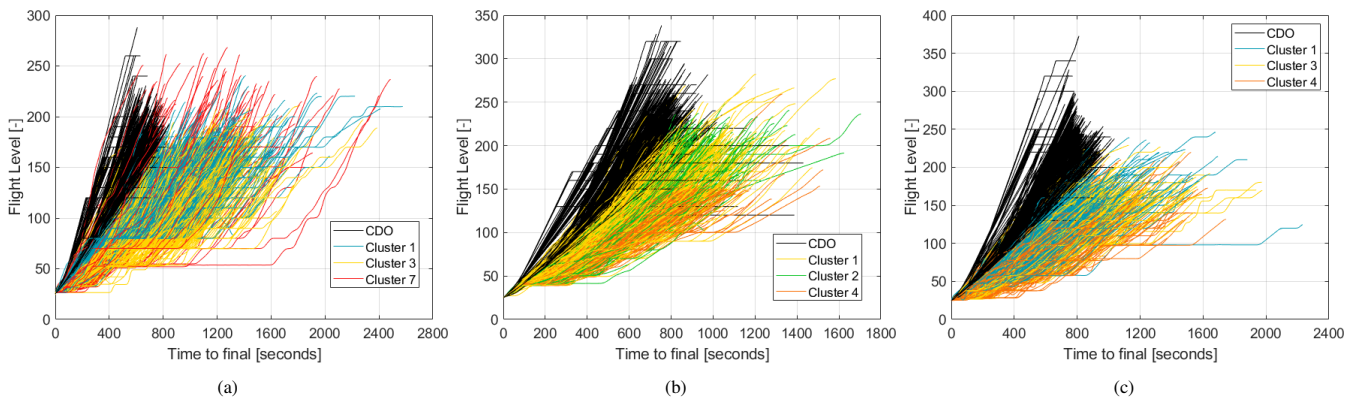


Figure 3. Vertical profiles of the actual flights for selected clusters, and reference CDOs (RT2), for EIDW (a), ESSA (b) and LOWW (c).

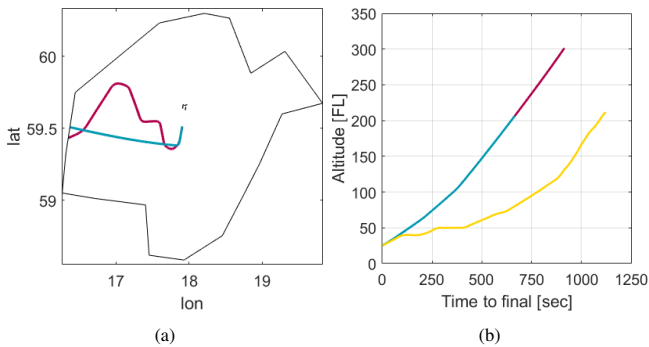


Figure 4. Example of horizontal (a) and vertical trajectories (b) for RT1 (red), RT2 (blue) and real flight (yellow), for an arrival in Stockholm TMA. Note that the horizontal trajectory of the real flight coincides with the one for RT1 (red).

that RT1 spends more time in TMA and thus, crosses the TMA border at a higher altitude.

When calculating the vertical reference trajectories, we assume an unrestricted descent, hence, we do not respect any altitude restrictions that may apply in the TMA. However, we

do not allow our vertical reference trajectories to cross the TMA border at a higher altitude than the cruise altitude for the flight, thus, we may have an initial level flight segment for flights that have a low cruise altitude.

Then, we use the obtained RT1 vertical reference trajectory as defined in [3], to calculate the **Vertical Deviation from the Reference Profile** metric as a function of time to final, and the area under the curve measured in $ft \cdot minutes$ constitutes our metric. Note that using RT2 as a reference trajectory would result in almost identical result as with RT1 as the only difference in the reference trajectories is their length, and different ground speed due to wind variations at different locations in TMA.

C. Additional Fuel Burn

We calculate the **Additional Fuel Burn** as the difference between the fuel consumption calculated for the real and the reference trajectories RT1 and RT2. For the real flights, we use the Total Energy Model (TEM) from BADA to find the thrust force, from which we can derive the thrust coefficient. As for the vertical reference trajectories, we use actual wind and temperature data from ERA5 [25]. To ensure the calculated

thrust stays within the feasible limits, we use BADA formulas for computing the thrust at the maximum climb rating and idle rating, which bound the thrust value from below and above. We do not take into account the effects of deploying flaps at lower speeds, which will generate more drag and increase the fuel consumption.

To estimate the fuel consumption, we derive the fuel coefficient from the thrust coefficient of the real trajectories, and for RT1 and RT2, we calculate the idle thrust fuel coefficient. We use the fuel coefficients (C_F) in the following equation to obtain the fuel flow per second, along each step of the trajectories:

$$F = \delta \cdot \theta^{\frac{1}{2}} \cdot m \cdot g_0 \cdot a_0 \cdot L_{HV}^{-1} \cdot C_F \quad (1)$$

Here, δ is the pressure ratio, θ is the temperature ratio, m is the reference mass, g_0 is the gravitational acceleration, a_0 is the speed of sound at sea level and L_{HV}^{-1} is the fuel lower heating value.

After having obtained the fuel flow per second, we use it in combination with the time in TMA for each trajectory to obtain the total fuel consumption, and the additional fuel burn when compared to RT1 and RT2.

D. Entry Conditions

The entry conditions are captured through the **Metering Effort** introduced in [19], [26]. Here we refer to the final metering, in oppose to the initial metering, which may take place in the en-route sectors typically with the support of arrival manager. The Metering Effort is defined as the difference of throughput at different time horizons, typically between entry and final. It is an indication of the level of traffic metering (or bunching) compared to the arrival capacity, and could also be a proxy for controller workload. For instance, a null value would correspond to a traffic perfectly metered, while a non-null value would reflect a non-metered traffic. The metering effort, as well as the throughput, relies on the construction of the minimum times to final heatmaps.

Minimum Time to Final. First, we plot all the flown trajectories of the given dataset. We overlay a rectangular grid with square cells (the length of the cell side 1 NM) over the TMA and calculate the minimum time to final for each cell of the grid, as the minimum time needed from any point within the cell of the grid to the final approach along any of the aircraft trajectories passing through the cell. We assign infinite (or a very large value) of the minimum time to final to the cells through which no trajectories pass during the considered time period. For visualisation of the resulting assignment, we plot a heatmap of the minimum time to final on a grid.

Throughput. The throughput at a given time horizon t is calculated by counting the number of aircraft with the minimum time to final within a given time window. In this work, we calculate the throughput crossing iso-minimum time lines from 600 to 30s to final, sampled at a 30s rate over the 5-minute periods (window width of 5 minutes, sliding by 30s steps). Figure 5 illustrates an example throughput plot and the corresponding metering effort.

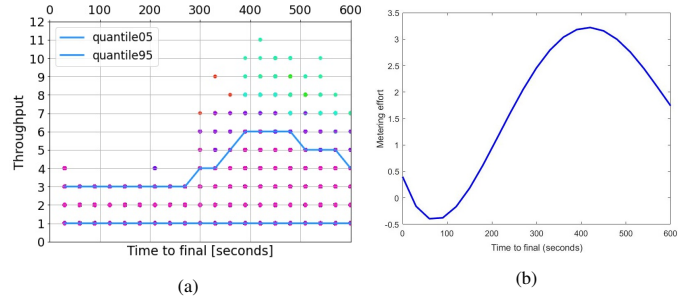


Figure 5. Example Throughput and the corresponding Metering Effort plots.

VI. RESULTS

We present the results of the performance evaluation, complemented by a detailed analysis per arrival flow. The flight efficiency graphs are presented in Figure 6; the entry conditions in Figures 7, 8 and 9; and the analysis per flow graphs in Figure 10.

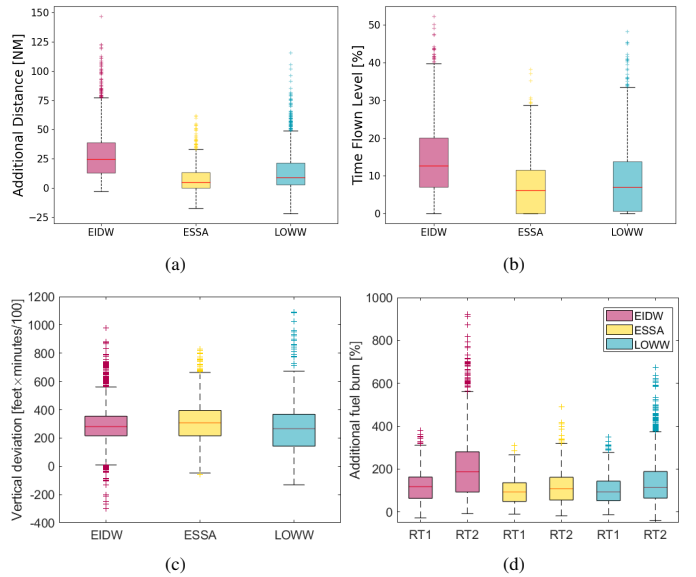


Figure 6. Additional Distance (a), Time Flown Level (b), Vertical Deviation from CDO (c) and Additional Fuel Burn calculated in respect to RT1 and RT2 (d) for the datasets representing EIDW, ESSA and LOWW airport arrivals.

1) Horizontal Flight Efficiency: For ESSA, the median **Additional Distance** is rather small (4.99 NM) (Figure 6a), which is consistent with the view of the trajectories that are mostly direct or with limited path extension (Figure 2). For LOWW, the value is slightly higher (8.79 NM) and with larger variance, consistent with the more pronounced path extension along the trombone legs. For EIDW, the Additional Distance is higher (24.86 NM), and is visible with the extensive use of the point merge arcs sometimes preceded by holding stacks for some flows. All this suggests an effect of the entry conditions in the terminal area.

For EIDW, the **Horizontal Spread** of 64% points out to the relatively low dispersion in the arrival flows, which mainly

follow the same paths and adhere to the procedures. For ESSA, it is 59%, suggesting a relatively low flow dispersion, with the holding patterns organized quite far from the runway (around the entry points to TMA), leaving almost half of the airspace for in-flight trajectory changes and manoeuvres. For LOWW, the Horizontal Spread is around 84%, suggesting a rather larger area of dispersion, with possible effect in terms of area of attention for the controller, airspace available for departures, and possible nuisance at low altitudes. Further analysis would be required to understand the effects of the different Horizontal Spreads.

2) *Vertical Flight Efficiency: Average Time Flown Level* expressed in percent of the flight time, suggests similar disposition (as the Additional Distance) for the three airports (see Figure 6b) with ESSA having the smallest value and EIDW the highest. Interestingly, the **Vertical Deviation** reveals a slightly different situation with the three airports with rather similar median values (in ft-minutes: 28130 for EIDW, 30730 for ESSA and 26590 for LOWW). This may suggest that while EIDW has the highest Time Flown Level (holding stacks and point merge arcs), when aircraft are in descent, their profile is closer to a continuous descent (typically when leaving the arcs) than for ESSA or LOWW.³

3) *Fuel Efficiency:* For the **Additional Fuel Burn** (Figure 6d) with the two reference horizontal trajectories (RT1 actual and RT2 ideal), the highest values are for Dublin (118% for RT1 and 187% for RT2, corresponding respectively to 147kg and 176kg), followed by Vienna (93% for RT1 and 114% for RT2, corresponding to 96kg and 104kg), while Arlanda shows the smallest values (93% for RT1 and 108% for RT2, corresponding to 97kg and 104kg). The difference among the airports for RT1 may be due to the level-offs (longer for EIDW, shorter for ESSA). The difference for RT2 may be caused by the additional distance (higher for EIDW, lower for ESSA), which seems to be a significant contributing factor.

We may note negative additional fuel burn occurrences, meaning that the fuel consumption of the real flight was lower than that of one of the reference. For Arlanda and Dublin, this is mostly caused by turboprop aircraft following the reference CDOs, spend more time in cruise inside the TMA, caused by a later top of descent (ToD) and a steeper descent trajectory. For Vienna, we observe the same phenomenon only for a couple of jet aircraft, operating short domestic flights where parts of the cruise phase is inside the TMA. Negative results obtained for RT2 may occur when the horizontal reference trajectory is longer than the real trajectory, which, for example, happens when the aircraft turns earlier for a shorter final approach, compared to that of the reference trajectory. Furthermore, due to the fact that we cluster aircraft trajectories and create a horizontal reference trajectory per cluster, the starting point of the reference trajectory along the TMA border may be farther from the airport than the actual point where the aircraft entered

³We have to remember also the possible sensitivity of the Time Flown Level indicator to the thresholds selected (30s leveloff and altitude difference of 300ft) versus the data accuracy.

the TMA, resulting in negative additional fuel burn if the real flight performed close to a CDO.

It should be noted that the computational time for calculation of the fuel burn range from 2.5 hours for Stockholm Arlanda to 6.5 hours for Dublin airport, performed on a laptop device with 15 Gb RAM and Intel i7-8565U CPU.

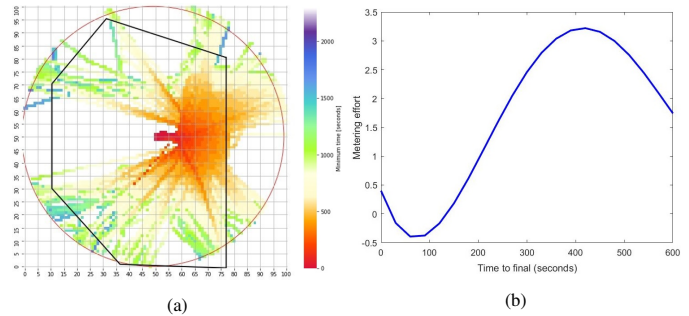


Figure 7. Minimum Time to Final heatmap (a) and Metering Effort (b) for the dataset representing the EIDW airport arrivals.

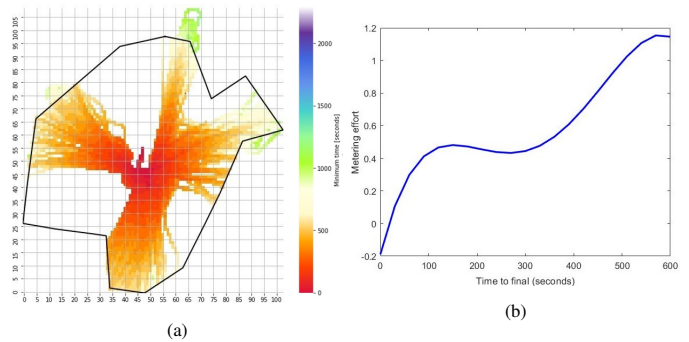


Figure 8. Minimum Time to Final heatmap (a) and Metering Effort (b) for the dataset representing the ESSA airport arrivals.

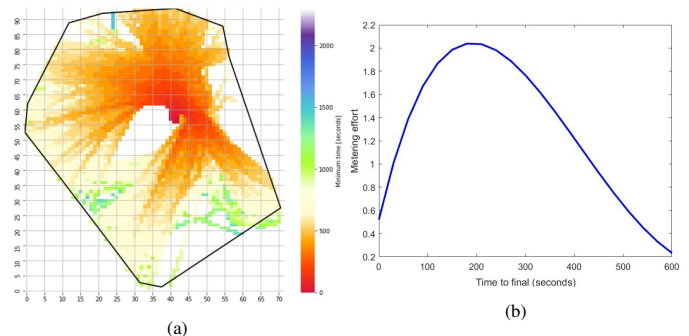


Figure 9. Minimum Time to Final heatmap (a) and Metering Effort (b) for the dataset representing the LOWW airport arrivals.

4) *Entry Conditions:* Figures 7, 8 and 9 show the heatmaps for the Minimum Times to Final and the Metering Effort at the three airports. For the calculation of these metrics we use a powerful Tetralith server [27], utilizing Intel HNS2600BPB computer nodes with 32 CPU cores, 384 GB, provided by the Swedish National Infrastructure for Computing (SNIC). The

computational times range from 8 hours (ESSA) to 2.2 days (EIDW).

The maximum values of the Minimum Times to Final vary among the airports: while for ESSA and LOWW they reach 1400 s, for EIDW it exceeds 2000 s, which is consistent with the high values of the Additional Distance in TMA.

For EIDW, the maximum Metering effort is observed at around 450s time to final with the value exceeding 3. This value corresponds to a number of flights, and represents the difference of the spread (5%-95% containment) of the throughput between 450s and 30s (final), considering a 5-minute time window. The target throughput is reached when the metering effort is zero, here around 150s.

For ESSA, the maximum Metering effort is at 600s with a value of 1.2. There is a first decrease, and then the final one with zero reached quite close to final. For LOWW, the Metering Effort goes up to 2 at around 200s then decreases, almost reaching zero. These three figures of Metering effort indicate significant differences of entry conditions among the airports, with the traffic samples considered. Obviously, for a given airport, a higher or lower traffic would lead to a different effort value. Here we may notice that EIDW is having by far the highest effort (3), followed by LOWW (2) and then ESSA (1.2). This should be taken into consideration when comparing flight efficiency.

5) *Flight Efficiency Per Cluster*: The Additional Fuel Burn per cluster, calculated with respect to RT1 and RT2, as well as Additional Distance and Time Flown Level are presented in Figure 10. (For cluster numbering, refer to Figure 2). We choose to analyse these three performance metrics together to get a better understanding of the sources of fuel inefficiencies.

When analysing the difference in additional fuel burn for the two reference trajectories RT1 and RT2, one should keep in mind that the similar values of the Additional Fuel Burn means that the distance corresponding to RT1 and RT2 is the same. For example, for Arlanda cluster 3 we observe a noticeable difference in the additional fuel burn calculated for RT1 and RT2, corresponding to the relatively high value of the Additional Distance and a moderate Time Flown Level, which may indicate that horizontal inefficiencies contribute significantly to the extra fuel consumption in this cluster. Similar trend is observed in multiple other clusters at our three airports: for Dublin clusters 1 and 5, we observe a very high difference in the Additional Fuel Burn for RT1 and RT2, which is accompanied by a high Additional Distance.

An example where vertical inefficiencies contribute more to the fuel loss is in Arlanda cluster 5, where the difference in additional fuel burn between RT1 and RT2 is small, but the absolute value of this metric is over 100%. The corresponding relatively low values in Additional Distance in TMA for this cluster, but relatively higher Time Flown Level, indicate that the fuel inefficiencies for this flow are mostly caused by inefficient vertical profiles.

Vienna cluster 4 shows a negative difference in additional fuel burn for RT1 and RT2, indicating that the horizontal trajectories of RT1 are shorter than those of RT2, which is

confirmed by the the low Additional Distance. The high additional fuel burn is mostly caused by vertical inefficiency, which we observe in the Time Flown Level. Another interesting observation in Vienna is that with similar fuel efficiency and Time Flown Level for clusters 3 and 4, we observe higher Additional Distance value for cluster 3, which is confirmed by higher difference between the additional fuel burn calculated for RT1 and RT2, than in cluster 4.

For Dublin cluster 8, we observe a very high difference in the Additional Fuel Burn calculated for RT1 and RT2. Here quite a low additional fuel burn value for RT1 would normally indicate good vertical performance, but the Time Flown Level reveals that vertical inefficiency exists. More detailed data analysis for this cluster uncovers, that there are mostly turboprop aircraft arriving from that direction, which cruise at a lower altitude than jet aircraft. This results in the later ToD for RT1, due to a more efficient vertical trajectory during descent, hence, the aircraft may be in cruise inside the TMA. This indicates that a vertically inefficient descent may result in less fuel spent in cruise, which yields the fuel consumption better than the reference one, obtained at an idle thrust setting. On the contrary, a later ToD, obtained when the vertical trajectory is steeper, may result in less fuel spent during descent but more fuel spent in cruise.

We suggest that such a targeted per-flow analysis helps to understand the sources of fuel inefficiencies within TMA, and identify the hotspots for further investigation.

VII. CONCLUSION AND FUTURE WORK

In this paper, we evaluate the arrival flight efficiency of Dublin, Stockholm-Arlanda and Vienna airports, using a set of metrics characterizing the horizontal, vertical and environmental efficiency, linking them to the metering effort and complementing the analysis with a more detailed per-flow evaluation, targeting a comprehensive view on the arrival operations in the terminal area.

The analysis reveals varied situations among the three airports. The median horizontal and vertical deviations range respectively from 5 to 25 NM, and from 26590 to 30730 ft-minutes; and the median additional fuel burn from 96 to 176 kg. However, these values cannot be compared without considering the entry conditions to the terminal area. Indeed, regardless of the final metering and sequencing technique involved, a terminal area subject to high bunches of traffic would be penalised compared to the one received a traffic metered by upstream sectors. Here, for the peak periods considered, the metering effort is ranging from 1.2 to 3, reflecting very different entry conditions among the three airports.

Further studies would be required to analyse flight efficiency under comparable entry conditions. Future work should also consider a breakdown of the two main sources of inefficiencies (airspace and operations) with a more detailed analysis taking into account the weather conditions as well as other sources of perturbations and uncertainties.

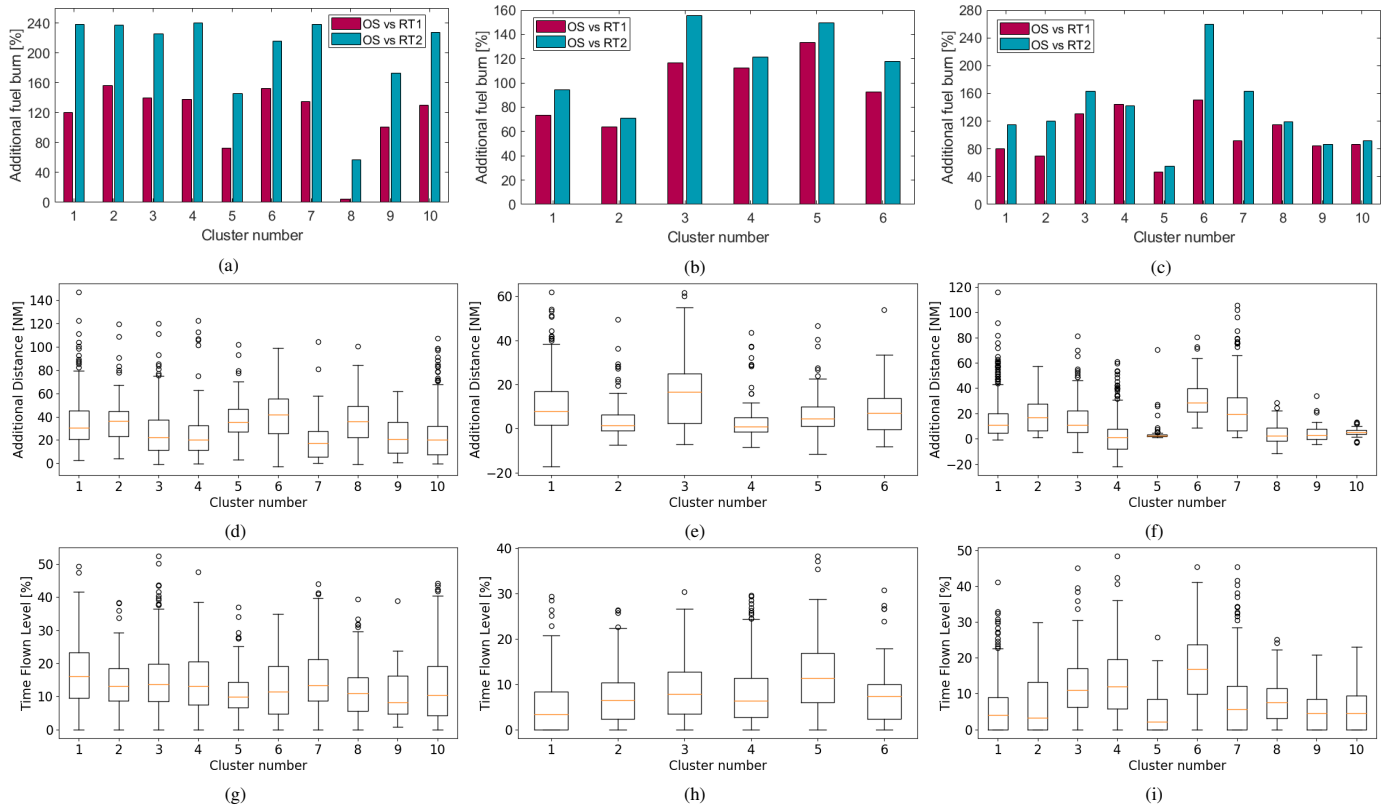


Figure 10. Additional Fuel Burn for the actual OpenSky (OS) trajectories compared to reference CDOs (a, b, c), Additional Distance (d, e, f) and Time Flown Level (g, h, i) per cluster, for EIDW, ESSA and LOWW respectively.

REFERENCES

- [1] “KPI Overview,” <https://www4.icao.int/ganportal/ASBU/KPI>, last accessed 20.01.2020.
- [2] “EUROCONTROL Performance Review Report: An Assessment of Air Traffic Management in Europe during the Calendar Year 2020.”
- [3] P. Pasutto, K. Zeghal, and E. G. Hoffman, “Flight inefficiency in descent: mapping where it happens,” in *AIAA AVIATION FORUM*, 2021.
- [4] G. B. Chatterji, “Fuel burn estimation using real track data,” in *ATTO 2011, including the AIAA Balloon Systems Conference and 19th AIAA Lighter-Than-Air Technology Conference*, p. 6881.
- [5] X. Prats, I. Agüi, F. Netjasov, G. Pavlovic, and A. Vidosavljevic, “APACHE-Final project results report,” 2018.
- [6] X. Prats, R. Dalmau, and C. Barrado, “Identifying the sources of flight inefficiency from historical aircraft trajectories,” in *ATM Seminar 2019*.
- [7] M. S. Ryerson, M. Hansen, and J. Bonn, “Time to burn: Flight delay, terminal efficiency, and fuel consumption in the national airspace system,” *Transportation Research Part A: Policy and Practice*, vol. 69, pp. 286–298, 2014.
- [8] H. Fricke, C. Seiss, and R. Herrmann, “Fuel and energy benchmark analysis of continuous descent operations,” in *ATM Seminar*, 2015.
- [9] F. Wubben and J. Busink, “Environmental Benefits of continuous descent approaches at Schiphol airport compared with conventional approach procedures,” National Aerospace Laboratory (NLR), Tech. Rep., 2000.
- [10] H. Hardell, T. Polishchuk, and L. Smetanova, “Fine-Grained Evaluation of Arrival Operations,” in *SIDs*, 2020.
- [11] A. Lemetti, T. Polishchuk, and H. Hardell, “Arrival Flight Efficiency in Numbers: What New the Covid-19 Crisis is Bringing to the Picture?” in *SIDs*, 2020.
- [12] EUROCONTROL, “Point Merge Implementation: A quick guide,” 2020.
- [13] “Irish AIP,” last accessed 08.10.2021. [Online]. Available: http://iaip.iaa.ie/iaip/aip_directory.htm/
- [14] “Austrian AIP,” last accessed 08.10.2021. [Online]. Available: <https://eaip.austrocontrol.at/>
- [15] Opensky Network, <https://opensky-network.org/>, last accessed 01.10.2020.
- [16] M. Schäfer, M. Strohmeier, V. Lenders, I. Martinovic, and M. Wilhelm, “Bringing Up OpenSky: A Large-scale ADS-B Sensor Network for Research,” in *IPSN’14*, 2014.
- [17] T. Polishchuk, A. Lemetti, and R. Saez, “Evaluation of Flight Efficiency for Stockholm Arlanda Airport using OpenSky Network Data,” in *OpenSky Workshop 2019*, ser. EPiC in Computing, vol. 67, pp. 13–24.
- [18] EUROCONTROL, “Analysis of Vertical Flight Efficiency During Climb and Descent,” 2017.
- [19] R. Christien, E. Hoffman, and K. Zeghal, “Towards a characterization of arrival metering, case study on a variety of european airports,” in *AIAA Aviation Forum*, 2020.
- [20] P. Pasutto, E. Hoffman, and K. Zeghal, “Vertical Efficiency in Descent Compared to Best Local Practices,” in *ATM Seminar*, 2019.
- [21] P. Pasutto, K. Zeghal, and E. G. Hoffman, “Vertical efficiency in descent: assessing the potential for improvements at the top 30 european airports,” in *AIAA AVIATION FORUM*, 2020.
- [22] V. Polishchuk, “Generating arrival routes with radius-to-fix functionalities,” in *ICRAT*, 2016.
- [23] H. Aksoy, E. T. Turgut, and Öznur Usanmaz, “The design and analysis of optimal descent profiles using real flight data,” *Transportation Research Part D: Transport and Environment*, vol. 100, p. 103028, 2021.
- [24] EUROCONTROL, “User Manual for the Base of Aircraft Data (BADA) Family 4,” 2014.
- [25] “Copernicus Climate Change Service (C3S) Data Store, European Centre for Medium-Range Weather Forecasts (ECMWF),” <https://cds.climate.copernicus.eu>, last accessed on 07.10.2021.
- [26] R. Christien, E. Hoffman, and K. Zeghal, “Spacing and Pressure to Characterise Arrival Sequencing,” in *ATM Seminar*, 2019.
- [27] “Tetralith server, NSC, Linköping University,” accessed on 28/09/2021. [Online]. Available: <https://www.nsc.liu.se/systems/tetralith/>